water

MDPI

Article

Spatial Downscaling of Satellite Precipitation Data in Humid Tropics Using a Site-Specific Seasonal Coefficient

Mohd. Rizaludin Mahmud [1,2,*], Mazlan Hashim [1,2], Hiroshi Matsuyama [3], Shinya Numata [3] and Tetsuro Hosaka [4]

1 Geoscience and Digital Earth Centre, Research Institute of Sustainability and Environment, Universiti Teknologi Malaysia, Skudai, Johor Bharu 81310, Malaysia; mazlanhashim@utm.my
2 Department of Geoinformation, Faculty of Geoinformation & Real Estate, Universiti Teknologi Malaysia, Skudai, Johor Bharu 81310, Malaysia
3 Faculty of Urban Environmental Sciences, Tokyo Metropolitan University, 1-1 Minami Osawa, Hachioji, Tokyo 192-0397, Japan; matuyama@tmu.ac.jp (H.M.); nmt@tmu.ac.jp (S.N.)
4 Graduate School for International Development and Cooperation, Hiroshima University, 1-5-1 Kagamiyama, Higashihiroshima 739-8529, Japan; hosaka3@hiroshima-u.ac.jp
* Correspondence: rizaludin@utm.my

Received: 11 February 2018; Accepted: 26 March 2018; Published: 31 March 2018

Abstract: This paper described the development of a spatial downscaling algorithm to produce finer grid resolution for satellite precipitation data (0.05°) in humid tropics. The grid resolution provided by satellite precipitation data (>0.25°) was unsuitable for practical hydrology and meteorology applications in the high hydrometeorological dynamics of Southeast Asia. Many downscaling algorithms have been developed based on significant seasonal relationships, without vegetation and climate conditions, which were inapplicable in humid, equatorial, and tropical regions. Therefore, we exploited the potential of the low variability of rainfall and monsoon characteristics (period, location, and intensity) on a local scale, as a proxy to downscale the satellite precipitation grid and its corresponding rainfall estimates. This study hypothesized that the ratio between the satellite precipitation and ground rainfall in the low-variance spatial rainfall pattern and seasonality region of humid tropics can be used as a coefficient (constant value) to spatially downscale future satellite precipitation datasets. The spatial downscaling process has two major phases: the first is the derivation of the high-resolution coefficient (0.05°), and the second is applying the coefficient to produce the high-resolution precipitation map. The first phase utilized the long-term bias records (1998–2008) between the high-resolution areal precipitation (0.05°) that was derived from dense network of ground precipitation data and re-gridded satellite precipitation data (0.05°) from the Tropical Rainfall Measuring Mission (TRMM) to produce the site-specific coefficient (SSC) for each individual pixel. The outcome of the spatial downscaling process managed to produce a higher resolution of the TRMM data from 0.25° to 0.05° with a lower bias (average: 18%). The trade-off for the process was a small decline in the correlation between TRMM and ground rainfall. Our results indicate that the SSC downscaled method can be used to spatially downscale satellite precipitation data in humid, tropical regions, where the seasonal rainfall is consistent.

Keywords: rainfall; monsoon; high resolution; TRMM

1. Introduction

Precise information on spatiotemporal rainfall is critical for accurate hydrology predictions and simulations in humid tropical regions. Satellite precipitation data are useful for supporting

in-situ measurements, because they provide wide coverage, are publicly available, and are grid-based. However, their suitability for small basins is hindered by their coarse grid size [1,2]. This is conspicuous for most humid tropical catchments in Southeast Asia, where the region comprises of small land–sea ration area—especially islands and peninsula. Hence, the spatial variability of tropical rainfall variation is rather high [3], and is expected to increase [4]. Although the new satellite precipitation data product from Global Precipitation Mission and GsMAP has higher resolution (0.1°) than its predecessor, the Tropical Rainfall Measuring Mission (TRMM), it is only available from 2015 onwards. Effective climate-hydrologic analysis requires continuous data, especially historical, and therefore it is important to improve those datasets. Due to that conflict, numerous efforts have been made to improve the coarse grids by spatial downscaling.

However, spatial-downscaling algorithms for satellite precipitation data for humid, tropical environments have rarely been reported. Currently, advances in spatial downscaling of satellite precipitation data are centered on using rainfall-related environmental parameters at higher spatial resolutions as predictors. Based on the strong relationship between the rainfall and its site-specific explanatory proxy variables, the rainfall values for a smaller grid were estimated through the regression coefficient. Often, multiple regression analyses are used to assess the relationships between rainfall, vegetation, and elevation [5–10]. Those variables were selected due to their significant relationship at a specific temporal period. In the temperate region, the relationship between seasonal rainfall and vegetation was strong, particularly during late spring and summer, where the photosynthetic rate increased. Meanwhile, topographic variations have significantly influenced regional or local rainfall patterns and distribution, especially in the hilly areas. These orographic effects can be relatively stronger if that region received air masses from the significant seasonal wind flows (e.g., monsoon).

Employing these variables for robust downscaling in humid tropical regions might be less suitable because of the weaker relationships between rainfall, vegetation, and elevation compared to temperate regions. Although applying multivariate regression could be effective in statistically increasing the predictive power of the model, the approach is constrained by several doubts: first is the possibility of a declining relationship between predictors and rainfall from low to finer resolution scales, and second is whether the high predictive power agreed with the physics of the rainfall-environmental perspectives [11–13]. Merging the rain gauge data to downscale the satellite precipitation in the tropics is useful, such as the process done by [14]. However, their method did not improved the spatial resolution of the precipitation. Efforts by [15] in applying the fractal downscaling is effective, but limited by the real-time support of wind and other meteorological data through complex processes. Therefore, an alternative initiative for an effective, operational, and less complex transformation of the satellite spatial downscaling in humid tropics is required.

The proxy variable in humid tropics should be one that influences rainfall patterns and, most importantly, one for which the surrogate data is available at a higher resolution than the satellite precipitation (<0.1°). Anders and Nesbitt [16] highlighted significant variables that influenced the satellite precipitation gradient in the tropics. On a local scale, precipitation was influenced by hydro-meteorological variables, namely prevailing winds, atmospheric moisture, and convective mode. Another important criteria for the spatial downscaling method is the operational aspect. Most of the satellite precipitation spatial downscaling models were developed based on the single or multivariate relationship over specific times and conditions; therefore, downscaling of the future satellite data requires the recalibration or redevelopment of the model, because either the predictor or the rainfall itself might change and influence the predictive power of the regression model (e.g., [8,15]).

Rainfall distribution in the tropics is closely associated with water vapor [17] and monsoons [18]. However, the high resolution data for water vapor is not available regularly, and therefore not suitable to be used as proxy downscaling variable. The Asian monsoon season contributed significantly to the variation in local rainfall in many tropical regions of Southeast Asia [19–21]. The seasonal rainfall pattern is found to be less variable on a local scale, and exhibits specific local zoning [21–23]. Using the ratio product between the satellite precipitation and the corresponding rain gauge to calibrate the

satellite precipitation is a well-developed approach in quantitative downscaling, and widely used in merging algorithms [24]. Theoretically, if the rainfall pattern was historically consistent over space and time, the ratio between the satellite and the rain gauge should follow a similar trend. We could expand this concept to developing a spatial downscaling method that is suitable for the humid tropics.

It is our aim to produce high-resolution satellite precipitation data by two process: first, by re-gridding the raw satellite precipitation data; and second, by recalculating the values of each pixel using the historical satellite–rain gauge ratio value. The appropriately high resolution would depend on two main factors: the density of rain gauges and the desired scale. For humid tropics, the challenge is to model atmospheric and hydro-meteorological variables at a mesoscale resolution (2–20 km) or lower [25,26]. We hypothesized that in humid tropical regions of low seasonal rainfall variability, the bias ratio between the previous satellite and ground measurements is consistent, and therefore can be used as a coefficient to estimate the accurate rainfall values of the future satellite precipitation datasets. If the site-specific coefficient were available at a smaller grid, a fine-scale estimation of the satellite precipitation would be achievable.

Based on the above-mentioned concept and hypothesis, we attempted to conduct an experiment. To test this hypothesis, Peninsular Malaysia was selected as an experimental site, because the coefficient of variance (COV) for seasonal precipitation is low [27]. The experiment has two main objectives: (1) Derive the site-specific coefficient (SSC) for each individual pixel, using the average bias ratio between the high-resolution ground rainfall data and re-gridded satellite rainfall data; and (2) validate the SSC to produce high-resolution precipitation maps. The proposed downscaling algorithm can be used to create high-resolution precipitation maps in the highly dynamic hydro-meteorological status quo of humid tropics, with less complex computation and more reliable results.

2. Materials and Methods

2.1. Study Site

Peninsular Malaysia (99.7–104.5° E, 1.3–6.8° N) is located in the western part of Malaysia (Figure 1a). It has a population of 18 million and an area of ~132,000 km^2. The general land cover is agricultural (52%), forest (22%), and built-up areas (26%) [28]. The climate is that of a tropical rainforest, with temperatures ranging from 24 °C to 32 °C and an annual rainfall of 2500 mm. The rainfall distribution pattern over Peninsular Malaysia is strongly influenced by seasonal monsoons, and the area is classified into five local climate regions: northwest, east, west, southwest, and highland (>400 m above sea level) (Figure 2) [27]. There are two distinct wet seasons: one from November to February, during which the northeast monsoon (NEM) produces heavy rainfall in the eastern region (Figure 1b); and the other from May until mid-September, when the southwest monsoon (SWM) affects areas in the west and southwest regions (Figure 1d). The northwest, west, and southwest regions experience two annual wet seasons, from mid-March until May (IM1) (Figure 1c), and from mid-September until August (IM2) [21,27]. Both of these seasons occur during the inter-monsoon periods between the NEM and SWM seasons. Substantial rainfall occurs during the inter-monsoon periods, because of the directional wind change and effects of the local topography.

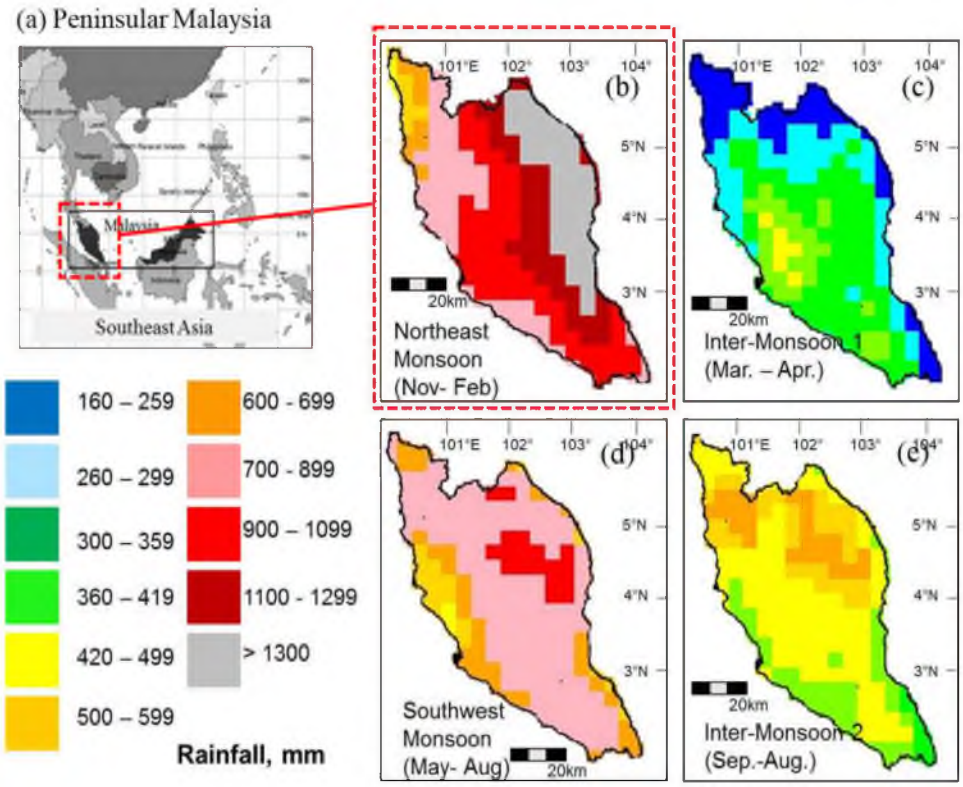

Figure 1. Peninsular Malaysia and its seasonal rainfall variation.

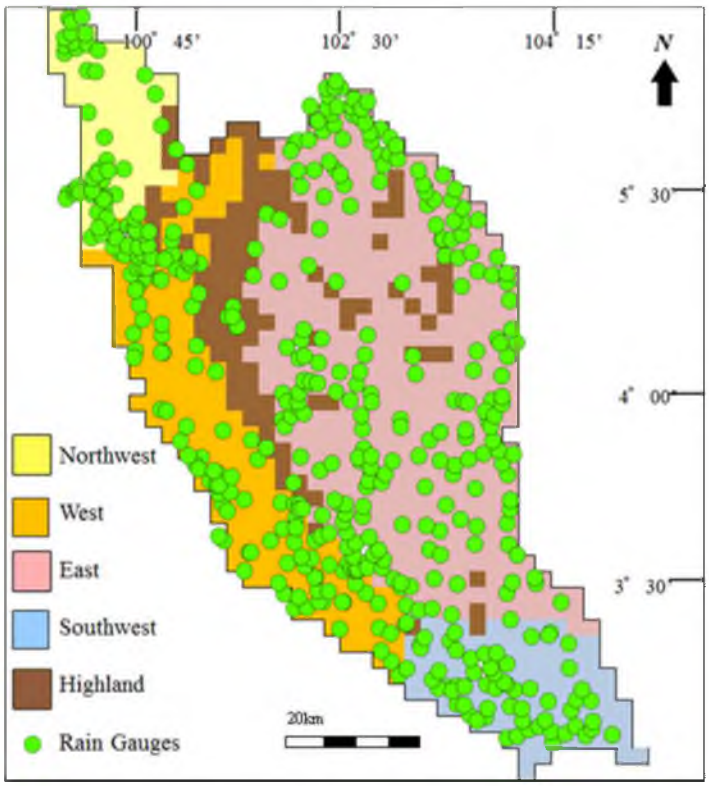

Figure 2. Rain gauge distribution in Peninsula Malaysia and rainfall zones (based on seasonal and intensity).

2.2. Data

2.2.1. Tropical Rainfall Measuring Mission Satellite Data

The Tropical Rainfall Measuring Mission (TRMM) Multi-Satellite Precipitation Analysis (TMPA) data product, which provides rainfall estimates from multiple satellites and other sources, was selected for this study. The TRMM satellite orbits the Earth at an altitude of 402 km, carrying three primary sensors, including precipitation radar (PR), a TRMM microwave imager (TMI), and a visible and infrared scanner (VIRS). The PR sensor is designed to provide detailed vertical distribution of radar reflectivity related to the amount of precipitation inside the system. The TMI sensor measures the vertically-integrated ice and water path, and the VIRS provides information on cloud-top temperatures and reflectance. Using the fundamental concept of precipitation and radar reflectivity, the rain rate is estimated. A general description of the data product, including algorithms and other parameters, can be found in the TRMM instruction manual (2005 and 2011).

Precipitation data products from the TRMM satellite were used because they provide frequent, current, and consistent data (scaling from three hourly to monthly readings) with high spatial resolution (0.25), and because the data are publicly available. The high spatial and temporal resolution satisfies the requirement of primary inputs for hydrological modelling and spatial analysis. The data were downloaded from the official website of the National Aeronautics and Space Administration (NASA), with the collaboration of the Japanese Aerospace Exploration Agency (JAXA). The rainfall data can be accessed from the following link (http://daac.gsfc.nasa.gov/data/datapool/TRMM/01_Data_Products/02_Gridded/index.html). The TMPA data for Peninsular Malaysia were extracted using the corresponding global coordinates for this region.

2.2.2. Rain Gauge Data

A total of 984 rain gauges, covering the entire Malaysia peninsula from 1998 (prior to the availability of the TRMM data) to 2011, were collected from the Malaysian Department of Irrigation and Drainage (Figure 2). Rain gauge measurements were conducted on a daily basis with a 24 h observation period, beginning and ending each day at 8:00 a.m. Then, the daily rainfall measurements were summed over one month to produce monthly rainfall data. After that, these data and their corresponding geographical coordinates were exported into a geographic information system (GIS) in shapefile format.

2.3. Downscaling Tropical Rainfall Measuring Mission Data Using the Seasonal Site-Specific Coefficient

2.3.1. Phase 1: Preparation of the High-Resolution Precipitation Data for Coefficient Derivation

Monthly areal precipitation at 0.05° resolution was generated using the dense rain gauge network and the universal co-kriging interpolation method in the ArcGIS software package (Esri, Redlands, CA, USA). Meanwhile, the satellite precipitation data was re-gridded from the original 0.25° resolution to a resolution of 0.05°, though within this new fine resolution grid (0.05°), the original precipitation value of the TRMM data was retained. For further understanding of this process, an illustration has been provided (Figure 3a). Two types of areal precipitation datasets were produced: the first is from the satellite; while the second is from the ground rain gauges, where both have an identical 0.05° grid. This process was done to the dataset from 1998 to 2008.

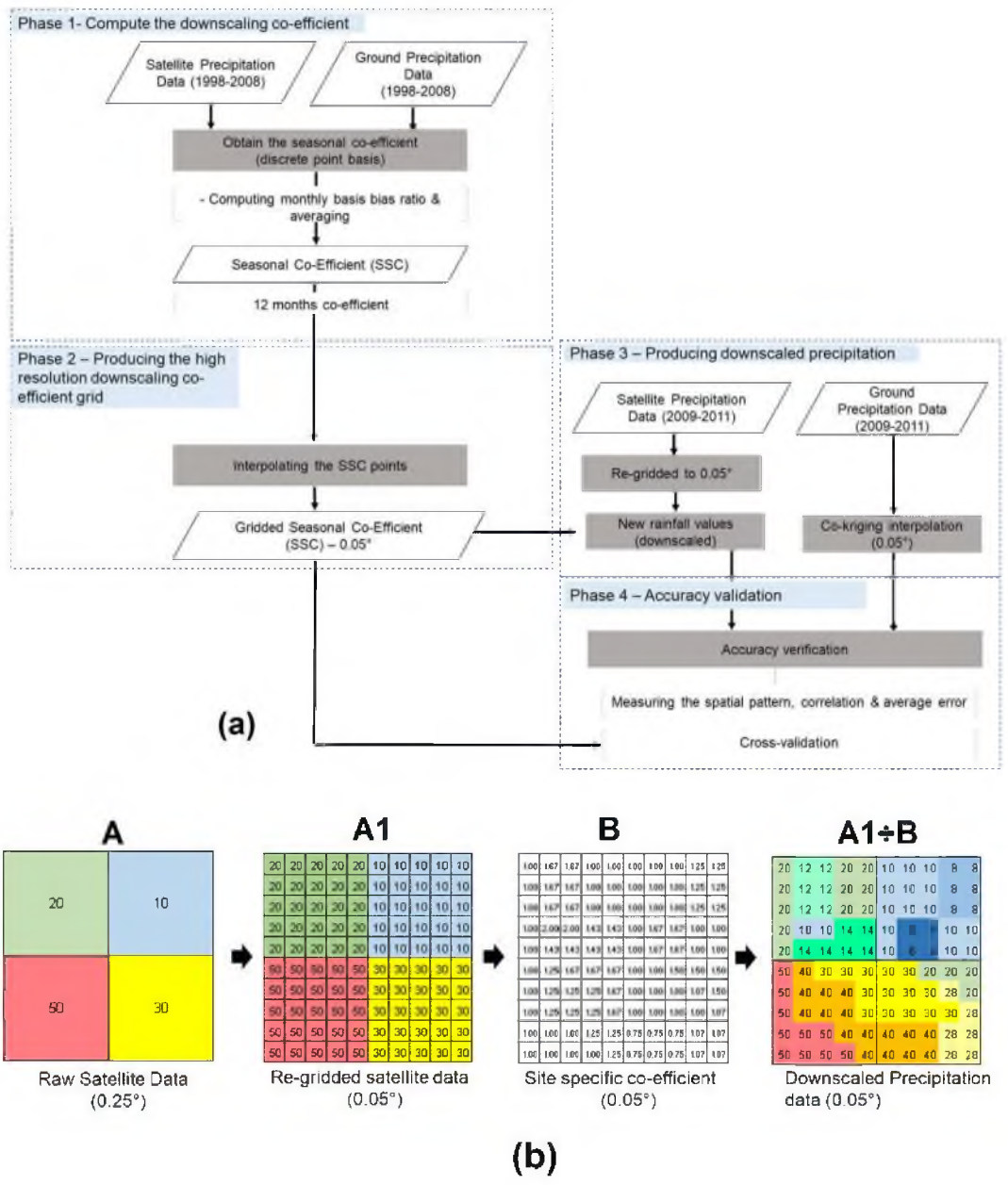

Figure 3. (**a**) Overall methodology. (**b**) Methodological flowchart of the spatial downscaling process—generating the high resolution precipitation data.

2.3.2. Phase 2: Deriving the Seasonal Site-Specific Coefficient

By using the input from phase 1, the SSC was derived through two fundamental steps. First, the re-gridded satellite precipitation data were divided by the ground precipitation. This process was performed at monthly scale. Prior to this process, new images were produced, where each pixel has a specific monthly bias ratio value. This was done for the dataset from 1998–2008. The second step was to calculate the average bias ratio for each pixel. The outcome of this process is known as the seasonal coefficient, or SSC. In total, there were 12 unique coefficient images, each representing the monthly basis downscale coefficient from January to December. Equation (1) shows the SSC-downscaled precipitation calculation, and Figure 3 illustrates the process (Phase 2).

$$HRC_{(i,j)} = \frac{1}{n}\sum \frac{Sat_{(i,j)}}{Rg_{(i,j)}} \quad (1)$$

$$DSat_{(i,j)} = \frac{RSat_{(i,j)}}{HRC_{(i,j)}} \quad (2)$$

where *Sat* is the satellite precipitation data, *Rg* is the areal ground precipitation data, *DSat* and *RSat* are the downscale and raw re-gridded precipitation values, respectively, and *i* and *j* are the pixel coordinates.

2.3.3. Phase 3: Downscaling the Tropical Rainfall Measuring Mission Satellite Data Using the Site-Specific Coefficient

The next step of the downscaling process is to apply the derived SSC to an independent dataset from 2009–2011. The satellite precipitation data was re-gridded from 0.25° to 0.05°. Subsequently, each pixel value for the re-gridded raw TRMM data (0.05°) was divided by the corresponding SSC derived in phase 2. An SSC value of 1.0 represents a perfect condition where no modification occurs. Meanwhile, an SSC value greater than 1.0 indicated an overestimate, and vice versa. Equations (1) and (2), as well as Figure 3 (phase 3), summarize the process of the SSC derivation and downscale process, respectively.

2.3.4. Phase 4: Accuracy Validation

To verify the performance of the SSC-downscale procedures, four indicators were used on their respective products, generated in phase 3. The first two indicators were the bias ratio reduction capacity and root mean square error (RMSE) between the precipitation product from the SSC-downscaled data and the interpolated rain gauges. To determine the quality of the SSC-downscaled products, we first computed the bias ratio reduction, which is the percent difference between the average bias ratios of the direct re-gridded raw TRMM data against that of the downscaled product. High bias ratio reduction capacity (~100%) indicated good quality (low bias), and vice versa. In addition, the coefficient of variance (COV) for the bias ratio was computed to examine whether the bias records were developed under low seasonal variance. Equation (3) shows the calculation for the bias ratio reduction capacity.

$$BR\ Capacity = \left(\frac{Bias\ ratio_{\overline{RSat}} - Bias\ ratio_{\overline{DSat}}}{Bias\ ratio_{\overline{RSat}}}\right) x\ 100\% \quad (3)$$

$$RMSE = \sqrt{\left[\frac{1}{N}\sum_{i=1}^{N}(S_i - G_i)^2\right]} \quad (4)$$

where *RSat* is the average of the directly re-gridded satellite precipitation data, *DSat* is the average SSC-based downscale precipitation, *Si* is the satellite precipitation, and *Gi* is the rain gauge measurement. RMSE was computed for two measurement pairs: downscale rainfall vs rain gauge, and raw rainfall vs rain gauge.

The third indicator was the bias ratio comparison to other gridded precipitation data products, measured either by satellite or rain gauge interpolation, or also by hybrids that are publicly available. This was carried out to determine the relative performance of the highest resolution of SSC-downscaled precipitation data upon other data products. Our expectation was that the SSC-downscaled should perform better than other products, or at least have comparable performance. Statistically, a small bias ratio was taken to indicate the spatial predictive increment after the downscaling process.

There were six gridded precipitation data products that were taken into account: (1) Global Satellite Mapping of Precipitation (GsMAP), (2) Precipitation Estimation from Remotely Sensed Information using Artificial Neural Networks (PERSIANN), (3) CPC Morphing precipitation product (CMORPH), (4) CPC Unified Gauge-Based Analysis of Daily Precipitation (CPC), (5) CPC Merged

Analysis Precipitation (CMAP) data, and (6) Global Precipitation Climatology Project (GPCP) precipitation data.

The GSMaP Project was sponsored by Japan Science and Technology—Core Research for Evolutional Science and Technology (JST-CREST) and is promoted by the JAXA Precipitation Measuring Mission (PMM) Science Team. The GsMAP products currently provide 0.1° resolution data, which is distributed by the Earth Observation Research Center, Japan Aerospace Exploration Agency [29]. The PERSIANN product, produced by the Center for Hydrometeorology and Remote Sensing (CHRS) at the University of California, uses neural network function classification procedures to compute an estimate of rainfall rate at 0.25° × 0.25° for each pixel of the infrared brightness temperature image provided by geostationary satellites [30]. Gridded precipitation numbers three to five were different types of products produced by the NOAA Climate Prediction Center, using various types of data and processing methods. The CPC product utilized the optimal interpolation (OI) objective analysis technique [31] provided by the NOAA Climate Prediction Center. Meanwhile, the CMORPH product produces high spatial and temporal resolution global precipitation estimates from passive microwave and infrared data. Morphing technique refers to the process of performing a time-weighting interpolation between multi-temporal, microwave-derived precipitation at a given location. Details about the morphing process can be found in [32]. Another product, CMAP, is a global precipitation product that merged precipitation estimates from several satellite-based algorithms and rain gauges. The creators of CMAP used the merging technique of reducing random error [33] and blending [34]. The last product, GPCP, eventually utilized a similar input, but with different merging techniques [24].

The fourth indicator was Moran's I. It was used to determine the qualitative performance of the downscaled result. Moran's I was able to define the rainfall pattern, and was reliable to be used in hydrology (e.g., [35]). The idea is that the pattern of the downscaled precipitation should more closely resemble the ground areal rainfall pattern. Therefore, the difference of the Moran's I values between the downscaled and ground areal rainfall should be small compared to those of the non-downscaled values. We computed the value based on monsoon preferences, because the rainfall patterns were strongly influenced by that factor. The corresponding equations [36] are shown below:

$$I = \frac{n \sum_{i=1}^{n} \sum_{j=1}^{n} w_{i,j} z_i z_j}{S_o \sum_{i=1}^{n} {z_i}^2} \quad (5)$$

$$S_o = \sum_{i=1}^{n} \sum_{j=1}^{n} w_{i,j} \quad (6)$$

where z_i is the rainfall value deviation from its mean, $w_{i,j}$ is the spatial weight between rainfall at i and j location, n is the total samples, and S_o is the aggregate of all the weights.

2.4. Determining the Effect of Interpolation to the Gridded Areal Ground Rainfall

To evaluate the effects of the interpolation process to the gridded site-specific coefficient, as well as the areal rainfall, k-fold cross-validation analysis was conducted. We applied the holdout method, which is based on separating the data into two sets: one is used for training and the other for testing. Prior to that, the rain gauge data was divided into two datasets. The samples for testing and validation were divided to be 60 and 40%, respectively. This is to ensure that there were a balanced number of samples between testing and validation, and also adequate samples to cover the whole study area [37]. A well-distributed selection was made to ensure the equivalent spatial coverage for both datasets. Two indicators were computed: the mean average error, known as root mean square error (RMSE); and the datasets' corresponding percentage against the average rainfall. We justified that the effect should be small and not affect the entire downscaling quality (<10%) [38].

3. Results

3.1. Performance of the Site-Specific Coefficient Tropical Rainfall Measuring Mission Downscaled Precipitation

(a) Quantitative Assessment

The three-year average showed that the SSC-TRMM downscaled precipitation had a lower bias ratio compared to the raw TRMM precipitation products over all hydro-climate regions (Table 1). The bias ratio reduction capacity is an indicator quantifying the effectiveness of the downscaling method in reducing bias, and represents high similarity value with the ground reference value, which had an average score of 54%. The greatest improvement was identified in the northwest, with a 94% bias reduction. Meanwhile, continuous performance over time showed that the downscaled precipitation data scored a lower RMSE compared to the raw precipitation data (Figure 4a–e). However, there was a slight decrease of the correlation between the downscaled precipitation data against the ground rainfall data. Nonetheless, it can be justified to be a very minimal effect. Hence, it can be considered as a positive trade-off, because the downscaled precipitation had improved the data's overall quality. The spatial refinement of factor five (from 0.25° to 0.05°) resulted in a remarkable improvement of the rainfall predictions, as indicated by a reduction in bias ratio of 54% and an RMSE of 40%.

Table 1. Bias ratio comparison between raw Tropical Rainfall Measuring Mission (TRMM) data and site-specific coefficient (SSC)-downscaled product.

Region	2009		2010		2011		Average Bias Ratio Reduction Capacity (%)	Average SSC Ratio *
	Raw	SSC	Raw	SSC	Raw	SSC		
Northwest	3.14	2.01	3.59	1.52	2.70	1.30	94	1.6
East	2.70	1.70	1.60	1.03	1.34	*0.86*	49	1.2
West	1.28	*0.83*	1.39	*0.85*	1.35	*0.84*	53	0.8
Southwest	1.45	1.09	2.16	1.57	1.72	1.31	31	1.3
Highland	1.04	*0.97*	1.43	*0.91*	1.35	*0.85*	41	0.9

* 1.0 is perfect ratio, >1.0 is a satellite overestimate, <1.0 is a satellite underestimate. The numbers in italics represent underestimate cases.

(b) Qualitative Assessment

From the qualitative perspective, a visual assessment showed that the spatial pattern of the SSC-downscaled precipitation more closely resembled the ground rainfall (Figure 5). This was statistically proven, where the differences between the Moran's I value of the downscaled precipitation and rain gauge-interpolated rainfall surfaces was getting smaller (Table 2). The corresponding average difference was 2%. Meanwhile, the average difference was 6% for the raw TRMM precipitation vs rain gauge-interpolated precipitation. These findings clarified that qualitatively, the SSC-downscaled precipitation was effective in depicting the actual rainfall on the ground compared to the raw version of the TRMM precipitation. Combining the results from quantitative and qualitative assessment showed that the overall SSC-downscaled precipitation results were able to precisely depict the actual ground rainfall over continuous spatial dimension and time, with a trade-off in decreased monthly correlation.

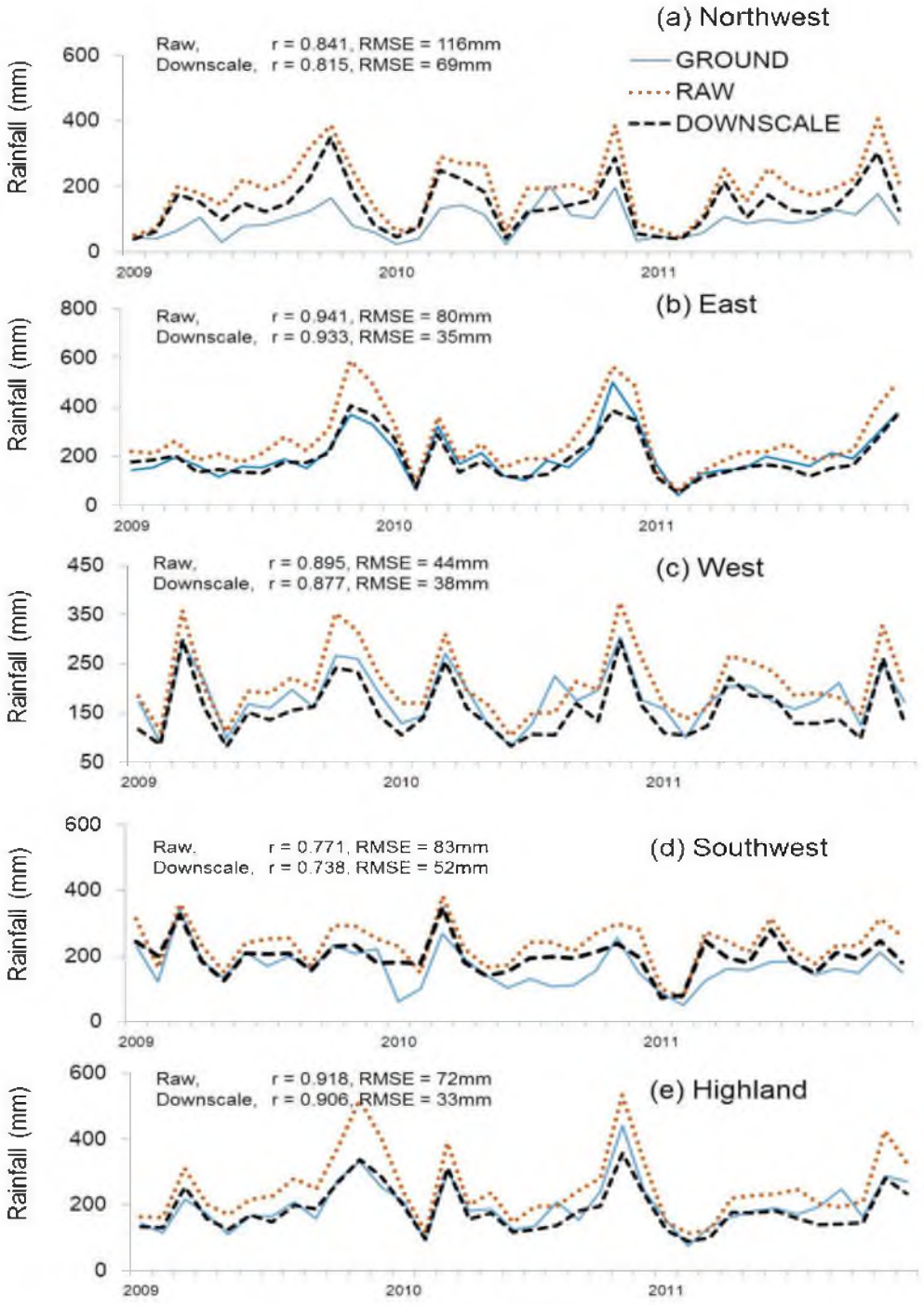

Figure 4. *Cont.*

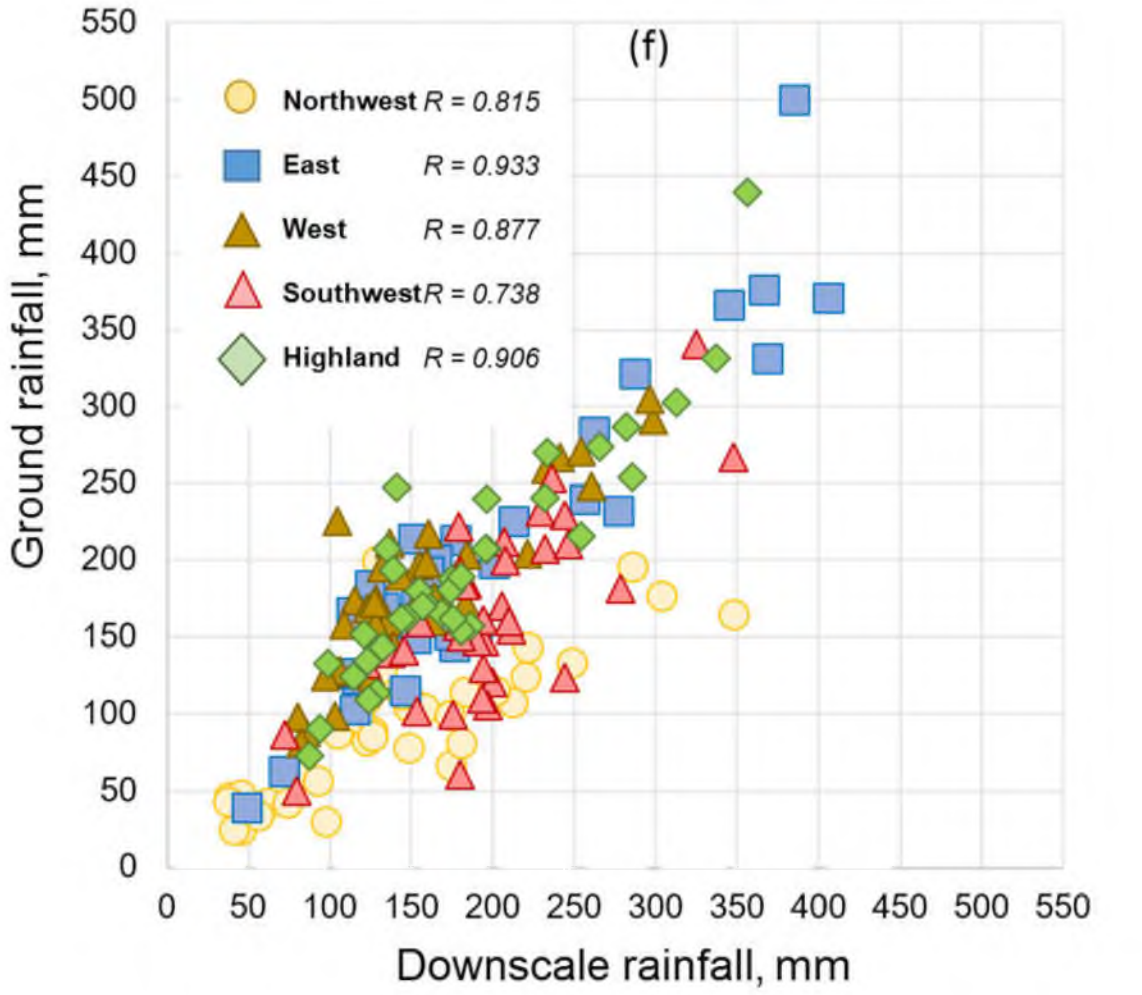

Figure 4. Time series between the ground areal rainfall, raw TRMM, and the SSC-downscale product from 2009–2011.

Table 2. Spatial autocorrelation of Moran's I value (transformed into a Z-score) of the interpolated rain gauge data (reference), raw TRMM, and the downscaled TRMM data.

Monsoon Season	Rain Gauge-Interpolated (a)	SSC-Downscale TRMM (b)	Raw TRMM (c)	Differences (%)	
				$(\|\|a - b\|\|/a) \times 100$	$(\|\|a - c\|\|/a) \times 100$
NEM	36.75	35.35	37.22	3.8	1.3
IM1	33.80	33.49	36.14	0.9	6.9
SWM	33.81	33.50	31.44	0.9	7.0
IM2	34.73	33.49	30.74	3.6	11.5

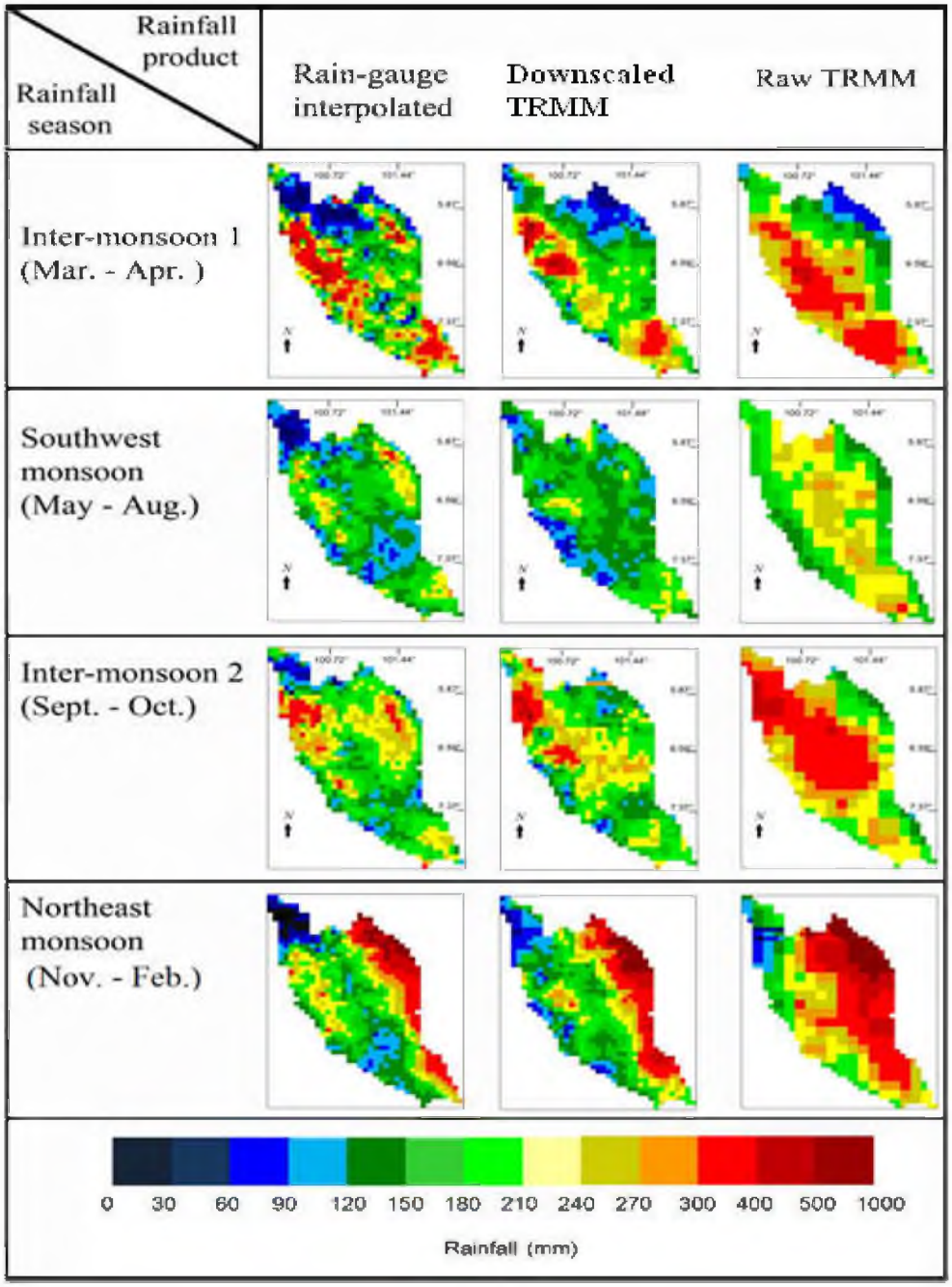

Figure 5. Seasonal rainfall maps of Peninsular Malaysia, from the interpolated rain gauge, site-specific coefficient-downscaled TRMM product, and raw TRMM product.

3.2. Coefficient of Variance of Historical Bias Ratio Records and Downscaling Performance

Hypothetically, the COV of the bias ratio records, which were the basis of the downscaling coefficient, should have a low variance (<35%). This 35% threshold as borrowed from [27], who used this value to classify the local hydro-climatic zone over the Malaysian peninsula. The regional average COV between the satellite and ground rainfall data was 37%, slightly higher than the preferred threshold. Nevertheless, this value was contributed by the large COV in the northwest (54%), while the other regions had relatively lower COV values (east: 34%; west: 34%; southwest: 31%; highland: 36%). One significant observation was that the COV was higher during the dry season, which takes place in February, in all regions (Figure 6). This finding showed that most of the downscaling coefficient was

derived under a low-variance bias (<35%), except in February. Nevertheless, we found no evidence or trend that related the low-variance condition of the downscaling coefficient and the effectiveness of the result. Therefore, the results of the lower bias might be achieved due to the site-specific coefficient, which minimized the bias in a robust fashion.

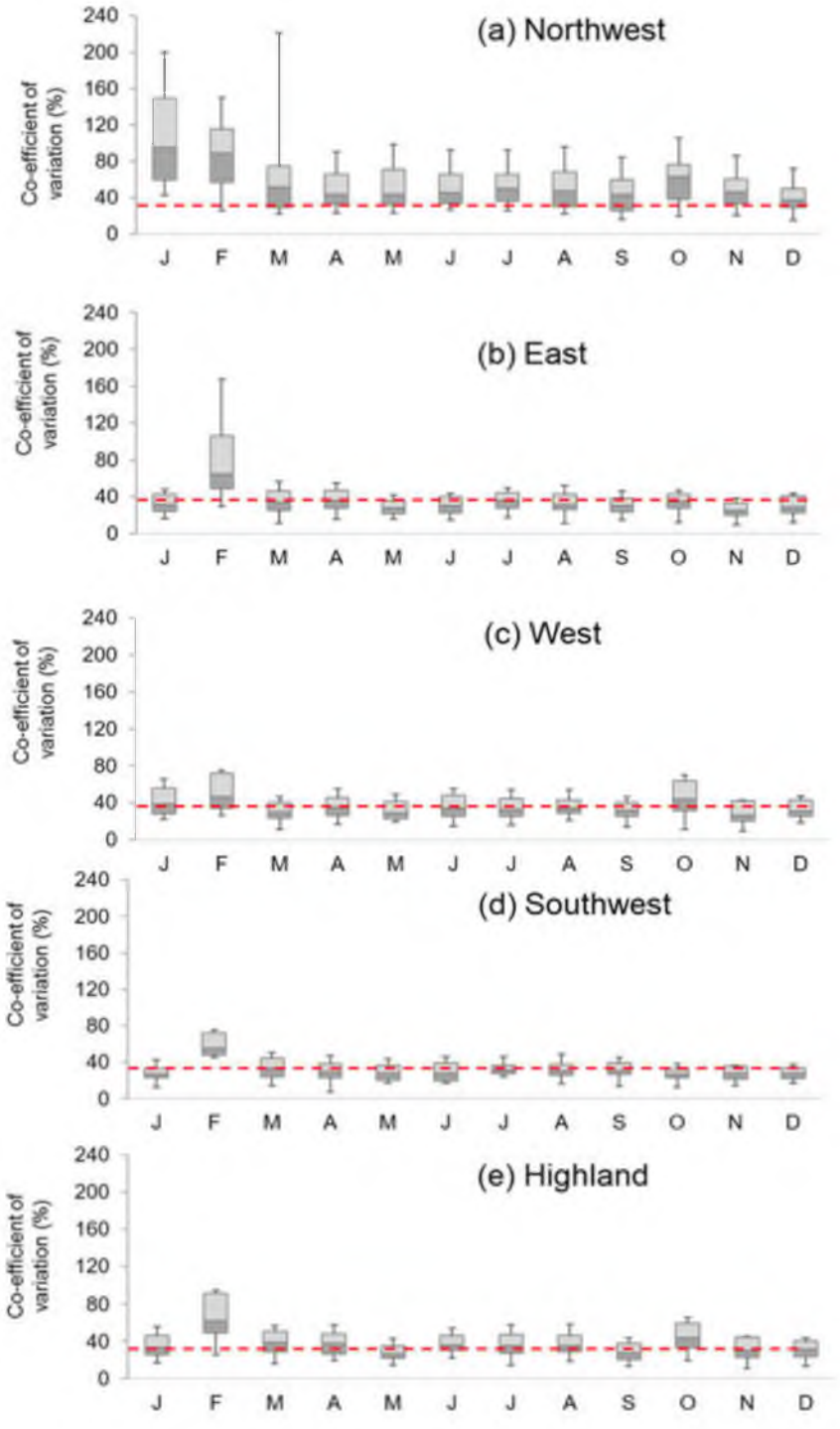

Figure 6. Coefficient of variance of the historical bias record, from the satellite and ground areal rainfall. The red line represents 35%, the threshold value for low variance.

3.3. Comparison of the Site-Specific Coefficient-Downscale and Other Satellite Precipitation Products

Discrete rain gauge comparison between the other satellite precipitation products were conducted, in order to determine the relative effectiveness of the SSC-downscaled precipitation. At the peninsular scale, the SSC-TRMM downscaled precipitation had a lower bias ratio than the other satellite precipitation products (Table 3). Only in the northwest and southwest did the GsMAP outperform the SSC-downscaled precipitation. However, the resolution of the GsMAP was relatively coarser (0.1°). We also found that the higher resolution of the SSC-TRMM-downscaled precipitation (<0.05°) was relatively better for depicting the local spatial rainfall in the western region, where many other precipitation products had failed to represent it.

Table 3. Comparison between the SSC-downscale product and other satellite precipitation products. N represents northwest, E is east, W is west, S is southwest, and H is highland.

Satellite Precipitation Products *	Grid Size (Deg.)	Ratio				
		N	E	W	S	H
TRMM V7—SSC	0.05	2.2	0.9	0.8	1.5	0.8
GsMAP	0.10	1.5	1.4	19.8	0.9	1.0
PERSIANN	0.25	15.0	1.8	43.5	1.9	1.4
CMORPH	0.25	10.6	1.8	20.5	2.0	1.3
CPC	0.50	21.0	1.9	23.7	1.4	0.8
GPCP	1.00	27.0	25.0	24.0	24.0	23.0
CMAP	2.50	15.0	1.8	43.5	1.9	1.4

* GsMAP: Global Satellite Mapping of Precipitation, PERSIANN: Precipitation Estimation from Remotely Sensed Information using Artificial Neural Networks, CMORPH: CPC Morphing Technique, CPC: Climate Prediction Centre Precipitation, GPCP: Global Precipitation Climatology Project, CMAP: CPC Merged Analysis of Precipitation.

3.4. Effects of the Interpolation Process

The cross-validation results showed that the interpolation scheme on both the SSC (Table 4) and ground areal rainfall were small (<10%) (Table 5). The very densely- and well-distributed samples could be the reason. A minor variation was found, where a higher error was indicated as rainfall intensity increased in specific monsoons. This minor effect was identified for interpolated ground rainfall. Nonetheless, we assumed that the interpolation process did not influence the results.

Table 4. Cross-validation analysis of the interpolated data. This evaluates the effect of interpolation to the derived site-specific coefficient. Zero percentage means that the interpolation has no effect to the value of the coefficient.

Monsoon Season	Cross-Validation Metrics
	MPE (%)
NEM (November–January)	5
IM1 (March–April)	3
SWM (May–August)	3
IM2 (September–October)	4
Average	4

Table 5. Ground areal rainfall (2009–2011). This result determines the effects of interpolation process to the ground areal rainfall, which was used in verifying the downscaled rainfall data from 2009–2011. Zero percentage of mean percentage error (MPE) means the interpolation process had no effect. RMSE is used in determining the quantitative effect of the interpolation in a standard unit (millimeters).

Monsoon Season	Cross-Validation Metrics		Average Ground Rainfall (mm)
	RMSE (mm)	MPE (%)	
NEM (November–January)	24	13	200
IM1 (March–April)	13	8	115
SWM (May–August)	11	9	118
IM2 (September–October)	21	10	176
Average	17	10	152

4. Discussion

The use of the SSC-downscaling method was able to produce a high-resolution precipitation map (0.05°) with improved quantitative accuracy. In addition, it was effective in spatially downscaling the future dataset without the input from rain gauges. Most of the present or previous merging, or other spatial resolution improvement methods, require multi-dataset or the ground in-situ preferences' surrogate information [5,6,24,32]. In the context of a tropical region, our results had a better performance compared to the downscaling based on multivariate regression done by [12] in mountainous, coastal, and forested environments. On the other hand, although our results' performance slightly underachieved in using the super ensemble method developed by Yatagai et al. (2014), we successfully produced higher-resolution precipitation data. Furthermore, our computation was less complex, and fewer input variables were required. Therefore, we can conclude that incorporating a dense rain gauge network [39], as well as monsoon rainfall seasonality and variability proved to be the effective in robustly downscaling satellite precipitation for various environmental contexts in the humid tropics.

Prior to positive results, this technique can be useful to the humid tropical regions, which have small land–sea ratio, many islands, and highly-variable seasonal rainfall patterns. Those characteristics are common and significant, especially for many areas in Southeast Asia [2,40,41]. It is also one of the regions in the world that receives large rainfall excess with high intensity [42], and is prone to extreme rainfall events [43]. The availability of high-resolution precipitation information would be significant for understanding the dynamics of tropical rainfall at a microscale.

In addition, smaller tropical catchment or sub-basin hydrology modelling from space will be possible. Current satellite precipitation data had limitations to representing the catchment scale rainfall, due to coarse resolution [2,44]. From a water resources perspective, with the availability of the global data, many humid tropical catchments for important reservoirs were categorized as smaller catchments (<10 km^2) [45]. They were located in thick, remote, and mountainous tropical forests, which are difficult to access. Utilizing an operational infrastructure could be expensive and laborious. Literature had showed that a substantial number of them were inadequately monitored and require support mechanisms [46,47].

Another positive implication of the downscaling method is the opportunity to develop higher-resolution historical tropical precipitation data from satellite datasets. This was a critical parameter that was missing from precise regional climate modelling, which is the primary domain of future climate and environmental sustainability efforts [25]. There were substantial amounts of coarse-resolution satellite precipitation data before TRMM, especially from the early METEOSAT missions [48–50]. Performing our SSC-downscaling technique to those datasets is plausible, under the condition that the site-specific coefficient should be derived first.

Despite the promising outcomes of this study, there were a few limitations. First was the requirement of a large rain gauge dataset. Because the downscaling coefficient was eventually derived

by correcting the bias factors at a smaller grid, it is necessary to have as large a rain gauge network as possible. This could be a limitation for hydrological data conflict areas (HDCS). An HDCS is an area which has experienced one or more of these conflicts: sparse rain gauges, missing rain gauge data, inefficient data sharing policies, or ineffective data management. The second limitation was whether the downscaling coefficient could be used for other satellite precipitation data besides TRMM. Hypothetically, it can be used, but a further investigation is needed.

The third limitation is that there was emerging evidence on the change in seasonal monsoon rainfall patterns, due namely to an external factor: El Nino Southern Oscillation (ENSO) [22,51,52]. This effect, however, was neglected in our study, due to lack of ENSO data at local scale. The final limitation was the effect of decreasing temporal correlation after the downscaling process. It was believed to be caused by the high-resolution output grid. Because the original TRMM gridded data was coarse, it tended to homogenize the local rainfall pattern. Therefore, as the grid was transformed to be smaller, the high heterogeneity of local rainfall patterns appeared. This effect, however, was minimal, and did not affect the output performance.

Anticipating the second and third limitations by testing the usability of the coefficient on other satellite precipitation data, and excluding samples that affected by ENSO, could be future work in to improve this study. In an effort to further localize the satellite precipitation data, utilizing the role of topographic control as a proxy variable is promising. This is especially true for high-altitude regions in the tropics. In addition, experimenting with the similar downscaling procedures at a higher temporal scale (i.e., weekly) could be worthwhile, because the rainfall in humid tropics is highly dynamic.

5. Conclusions

We tested the hypothesis that higher-resolution data on historical bias records for low-variance seasonal monsoon rainfall can be used to spatially downscale TRMM satellite precipitation data. The use of the site-specific coefficient successfully transformed the initial TRMM satellite precipitation data resolution from 0.25° to 0.05°, with smaller errors and increased similarity with the ground rainfall pattern. With the availability of the SSC, the downscaling of the future satellite precipitation data can be done without any ground reference or rain gauge data. However, it caused a small decline in the temporal correlation. The simplistic and effective procedure described in this study can be applied to spatially downscale satellite precipitation data in regions with low variability in seasonal rainfall in the humid tropics.

Acknowledgments: The authors would like to thanks all the stakeholders and respective agencies, particularly the Department of Irrigation and Drainage for their support regarding the in-situ data. Our utmost gratitude goes to Universiti Teknologi Malaysia and Ministry of Higher Education for supporting this study through the research grants (QJI30000.2727.02K83 and QJ130000.2427.04G12).

Author Contributions: Mazlan Hashim provides the datasets including the required supporting geoinformation software needed for the analyses; S. Numata, H. Matsuyama and T. Hosaka cooperated in designing and improving the concept of the research project and related processes; Mohd Rizaludin Mahmud conceived the research project, conducted the data processing and analysis. All the authors participated actively in preparing and reviewing the manuscript; moderated by Mohd Rizaludin Mahmud.

Conflicts of Interest: The authors declare no conflicts of interest

References

1. Behrangi, A.; Khakbaz, B.; Jaw, T.C.; AghaKouchak, A.; Hsu, K.; Sorooshian, S. Hydrologic evaluation of satellite precipitation products over a mid-size basin. *J. Hydrol.* **2011**, *360*, 225–237. [CrossRef]
2. Mahmud, M.R.; Numata, S.; Hosaka, T.; Matsuyama, H.; Hashim, M. Preliminary study for effective seasonal downscaling of TRMM precipitation data in Peninsular Malaysia: Local scale validation using high resolution areal precipitation. *Remote Sens.* **2015**, *7*, 4092–4111. [CrossRef]
3. Bidin, K.; Chappell, N.A. First evidence of a structured and dynamic spatial pattern of rainfall within a small humid tropical catchment. *Hydrol. Earth Syst. Sci.* **2003**, *7*, 245–253. [CrossRef]

4. Chadwick, R.; Boutle, I.; Martin, G. Spatial patterns of precipitation change in CMIP5: Why the rich do not get richer in the tropics. *J. Clim.* **2013**, *26*, 3803–3822. [CrossRef]
5. Chen, F.; Liu, Y.; Liu, Q.; Li, X. Spatial downscaling of TRMM 3B43 precipitation considering spatial heterogeneity. *Int. J. Remote Sens.* **2014**, *35*, 3074–3093. [CrossRef]
6. Cho, H.; Choi, M. Spatial downscaling of TRMM precipitation using MODIS product in the Korean Peninsula. In Proceedings of the AGU 2013 Fall Meeting, Francisco, CA, USA, 9–13 December 2013. Abstract, H43G-1537.
7. Immerzeel, W.W.; Rutten, M.M.; Droogers, P. Spatial downscaling of TRMM precipitation using vegetative response on the Iberian Peninsula. *Remote Sens. Environ.* **2009**, *113*, 362–370. [CrossRef]
8. Jian, F.; Du, J.; Xu, W.; Shi, P.; Li, M.; Ming, X. Spatial downscaling of TRMM data based on orographic effect and meteorological condition of mountainous region. *Adv. Water Resour.* **2013**, *61*, 42–50.
9. Park, N.-W. Spatial downscaling of TRMM precipitation using geostatistics and fine scale environmental variables. *Adv. Meteorol.* **2013**, *2013*, 1–8. [CrossRef]
10. Shi, Y.; Song, L.; Xia, Z.; Lin, Y.; Myeni, R.B.; Choi, S.; Was, L.; Ni, X.; Lao, C.; Yang, F. Mapping annual precipitation across mainland China in the period of 2001–2010 from TRMM 3B43 product using spatial downscaling approach. *Remote Sens.* **2015**, *7*, 5849–5878. [CrossRef]
11. Park, N.-W.; Kyriakidis, P.C.; Hong, S. Geostatistical integration of coarse resolution satellite precipitation products and rain gauge data to map precipitation at fine spatial resolutions. *Remote Sens.* **2017**, *9*, 255. [CrossRef]
12. Ulloa, J.; Ballari, D.; Campozano, L.; Samaniego, E. Two-step downscaling of TRMM 3B43 V7 precipitation in contrasting climatic regions with sparse monitoring: The case of Ecuador in tropical South America. *Remote Sens.* **2017**, *9*, 758. [CrossRef]
13. Zhang, Y.; Li, Y.; Ji, X.; Luo, X.; Li, X. Fine-Resolution Precipitation Mapping in a Mountainous Watershed: Geostatistical Downscaling of TRMM Products Based on Environmental Variables. *Remote Sens.* **2018**, *10*, 119. [CrossRef]
14. Yatagai, A.; Krishnamurti, T.N.; Kumar, V.; Mishra, A.K.; Simon, A. Use of APHRODITE rain gauge–based precipitation and TRMM 3B43 products for improving Asian monsoon seasonal precipitation forecasts by the superensemble method. *J. Clim.* **2014**, *27*, 1062–1069. [CrossRef]
15. Tao, K.; Barros, P. Using fractal downscaling of satellite precipitation products for hydrometeorological applications. *J. Atmos. Ocean. Technol.* **2010**, *27*, 409–427. [CrossRef]
16. Anders, A.; Nesbitt, S.W. Altitudinal precipitation gradients in the tropics from Tropical Rainfall Measuring Mission (TRMM) Precipitation Radar. *J. Hydrometeor.* **2015**, *16*, 441–448. [CrossRef]
17. Muller, C.J.; Back, L.E.; O'Gorman, P.A.; Emanuel, K.A. A model for the relationship between tropical precipitation and column water vapor. *Geophys. Res. Lett.* **2009**, *36*, L16804. [CrossRef]
18. Chang, C.; Ding, Y.; Lau, N.; Johnson, R.H.; Wang, B.; Yasunari, T. *The Global Monsoon System*; World Scientific Series on Asia-Pacific Weather and Climate; World Scientific: Singapore, 2011; Volume 5.
19. Lee, H.S. General rainfall patterns in Indonesia and the potential impacts of local season rainfall intensity. *Water* **2015**, *7*, 1751–1768. [CrossRef]
20. Singhrattna, N.; Rajagopalan, B.; Kumar, K.K.; Clark, M. Interannual and interdecadal variability of Thailand Summer Monsoon Season. *J. Clim.* **2005**, *18*, 1697–1708. [CrossRef]
21. Varikoden, H.; Preethi, B.; Samah, A.A.; Babu, C.A. Seasonal variation of rainfall characteristics in different intensity classes over Peninsular Malaysia. *J. Hydrol.* **2011**, *404*, 99–108. [CrossRef]
22. Aldrian, E.; Dumenil, G.L.; Widodo, F.H. Seasonal variability of Indonesian rainfall in ECHAM4 simulations and in the reanalyses: The role of ENSO. *Theor. Appl. Climatol.* **2007**, *87*, 41–59. [CrossRef]
23. Fein, J.S.; Stephens, P.L. *Monsoons*; John Wiley and Sons: New York, NY, USA, 1988.
24. Huffman, G.J.; Adler, R.F.; Arkin, P.; Chang, A.; Ferraro, R.; Gruber, A.; Janowiak, J.; Rudolf, B.; McNab, A.; Schneider, U. The Global Precipitation Climatology Project (GPCP) combined precipitation dataset. *Bull. Am. Meteorol. Soc.* **1997**, *78*, 5–20. [CrossRef]
25. Manzanas, R. Statistical downscaling in the tropics can be sensitive to reanalysis choice: A Case Study for Precipitation in the Philippines. *J. Clim.* **2015**, *28*, 4171–4184. [CrossRef]
26. Thompson, R.D. *Atmospheric Processes and Systems*, 1st ed.; Routledge: River Thames, UK, 1998.
27. Wong, C.L.; Venneker, R.; Uhlenbrook, S.; Jamil, A.B.M.; Zhou, Y. Variability of rainfall in Peninsular Malaysia. *Hydrol. Earth Syst. Discuss.* **2009**, *6*, 5471–5503. [CrossRef]

28. MACRES & UTM. *Satellite Atlas Malaysia*; Malaysian Centre for Remote Sensing: Kuala Lumpur, Malaysia, 2000.
29. Okamoto, K.; Iguchi, T.; Takahashi, N.; Iwanami, K.; Ushio, T. The Global Satellite Mapping of Precipitation (GSMaP) project. In Proceedings of the 2005 IEEE International Geoscience and Remote Sensing Symposium, Seoul, Korea, 25–29 July 2005; pp. 3414–3416.
30. Hsu, K.; Gao, X.; Sorooshian, S.; Gupta, H.V. Precipitation Estimation from Remotely Sensed Information Using Artificial Neural Networks. *J. Appl. Meteorol.* **1997**, *36*, 1176–1190. [CrossRef]
31. Chen, M.; Xie, P.; CPC Precipitation Working Group CPC/NCEP/NOAA. CPC Unified Gauge-based Analysis of Global Daily Precipitation. In Proceedings of the Western Pacific Geophysics Meeting, Cairns, Australia, 29 July–1 August 2008.
32. Joyce, R.J.; Janowiak, J.E.; Arkin, P.A.; Xie, P. CMORPH: A method that produces global precipitation estimates from passive microwave and infrared data at high spatial and temporal resolution. *J. Hydrometeorol.* **2004**, *5*, 487–503. [CrossRef]
33. Xie, P.; Arkin, P.A. Global precipitation: A 17-year monthly analysis based on gauge observations, satellite estimates, and numerical model outputs. *Bull. Am. Meteorol. Soc.* **1996**, *78*, 2539–2558. [CrossRef]
34. Reynolds, R.W. A real-time global sea surface temperature analysis. *J. Clim.* **1988**, *1*, 75–86. [CrossRef]
35. Wagesho, N.; Goel, N.K.; Jain, M.K. Temporal and spatial variability of annual and seasonal rainfall over Ethiopia. *Hydrol. Sci. J.* **2013**, *58*, 354–373. [CrossRef]
36. Mitchell, A. *The ESRI Guide to GIS Analysis*; ESRI Press: Redlands, CA, USA, 2005; Volume 2.
37. Hastie, T.; Tibshirani, R.; Friedman, J. *The Elements of Statistical Learning, Data Mining, Inference, and Prediction*, 2nd ed.; Springer: New York, NY, USA, 2001.
38. Mair, A.; Fares, A. Comparison of rainfall interpolation methods in a mountainous region of a tropical island. *J. Hydrol. Eng.* **2011**, *16*, 371–383. [CrossRef]
39. Krishnamurti, T.N.; Kishtawal, C.M.; Simon, A.; Yatagai, A. Use of a dense gauge network over India for improving blended TRMM products and downscaled weather models. *J. Meteorol. Soc. Jpn.* **2009**, *87*, 395–416. [CrossRef]
40. Prasetia, R.; As-syakur, A.R.; Osawa, T. Validation of TRMM precipitation radar satellite data over Indonesian region. *Theor. Appl. Climatol.* **2013**, *112*, 575–587. [CrossRef]
41. Roongroj, C.; Long, S.C. Thailand daily rainfall and comparison with TRMM products. *J. Hydrometeorol.* **2008**, *9*, 256–266.
42. Endo, N.; Jun Matsumoto, J.; Lwin, T. Trends in Precipitation Extremes over Southeast Asia. *SOLA* **2009**, *5*, 168–171. [CrossRef]
43. Ono, K.; Kazama, S. Analysis of extreme daily rainfall in Southeast Asia with a gridded daily rainfall data set. Hydro-climatology: Variability and Change In Proceedings of Symposium J-H02 Held During IUGG2011 in Melbourne, Melbourne, Australia, 28 June–7 July 2011; p. 344.
44. Mahmud, M.R.; Hashim, M.; Mohd Reba, M.N. How effective is the new generation of GPM satellite precipitation in characterizing the rainfall variability over Malaysia? *Asia-Pac. J. Atmos. Sci.* **2017**, *53*, 375–384. [CrossRef]
45. Sidle, R.C.; Tani, M.; Zeigler, A.D. Catchment processes in Southeast Asia: Atmospheric, hydrologic, erosion, nutrient cycling, and management effects. *For. Ecol. Manag.* **2006**, *224*, 1–4. [CrossRef]
46. Liu, X.; Liu, F.M.; Wang, X.X.; Li, X.D.; Fan, Y.Y.; Cai, S.X.; Ao, T.Q. Combining rainfall data from rain gauges and TRMM in hydrological modelling of Laotian data-sparse basins. *Appl. Water Sci.* **2017**, *7*, 1487–1496. [CrossRef]
47. Musiake, K. Hydrology and water resources in monsoon Asia: A consideration of the necessity of establishing a standing research community of hydrology and water resources in the Asia Pacific region. *Hydrol. Process.* **2003**, *17*, 2701–2709. [CrossRef]
48. Jobard, I.; Desbois, M. Satellite estimation of the tropical precipitation using the METEOSTAT and SSM/I data. *Atmos. Res.* **1994**, *34*, 285–298. [CrossRef]
49. Levizzani, V. Precipitation estimates using METEOSAT second generation (MSG): New perspectives from geostationary orbit. In Proceedings of the 1999 EUMETSAT meteorological Satellite Data users' Conference, Copenhagen, Denmark, 6–10 September 1999; pp. 121–128.
50. Turpeinin, O.M. Monitoring of precipitation with METEOSAT. *Adv. Space Res.* **1989**, *9*, 347–353. [CrossRef]

51. Hendon, H.H. Indonesian rainfall variability: Impacts of ENSO and local air-sea interaction. *J. Clim.* **2003**, *16*, 1775–1790. [CrossRef]
52. Loo, Y.Y.; Billa, L.; Singh, A. Effect of climate change on seasonal monsoon in Asia and its impact on the variability of monsoon rainfall in Southeast Asia. *Geosci. Front.* **2014**, *6*, 817–823. [CrossRef]